Düzce University
Journal of Science & Technology

MAO-A Inhibitor Properties by Molecular Modeling Method, Antimicrobial Activity and Characterization of Silver Nanoparticles Synthesized from *Lactifluus Bertillonii* Mushroom

Yasemin KEŞKEK KARABULUT [a,*], Aybek YİĞİT [b], Ayşe KARACALI TUNÇ [c], Büşra Merve SARITAŞ [d], Sedat KESİCİ [e], Yusuf UZUN [f], Cemil SADULLAHOĞLU [g]

[a] Project Development and Coordination Office, Rectorate, Kırklareli University, Kırklareli, TÜRKİYE
[b] Department of Pharmacy Services, Tuzluca Vocational School of Higher Education, Iğdır University, Iğdır, TÜRKİYE
[c] Health Care Vocational School of Higher Education, Iğdır University, Iğdır, TÜRKİYE
[d] Department of Dental Services, Health Care Vocational School of Higher Education, Iğdır University, Iğdır, TÜRKİYE
[e] Department of Plant and Animal Production, Yüksekova Vocational School of Higher Education, Hakkari University, Hakkari, TÜRKİYE
[f] Department of Pharmacy Professional Sciences, Faculty of Pharmacy, Van Yüzüncü Yıl University, Van, TÜRKİYE
[g] Department of Veterinary Medicine, İdil Vocational School of Higher Education, Şırnak University, Şırnak, TÜRKİYE
* Corresponding author's e-mail address: ykeskekkarabulut@klu.edu.tr
DOI: 10.29130/dubited.1445798

ABSTRACT

This work focuses on the antimicrobial activity of AgNPs produced using a green, environmentally friendly synthesis process from *Lactifluus bertillonii* mushrooms using the minimum inhibitory concentration (MIC) method. Additionally, the inhibitory characteristics of the chemicals present in the mushroom extract are also determined. SEM, TEM, UV-vis, and FT-IR instruments are employed as part of the study. The average particle size in the characterisation was determined by the imaging program to be 10.471 nm. Additionally, the activity of AgNPs against *Klebsiella pneumoniae* was found to be 512 µg/ml in the antimicrobial activity tests carried out using the MIC method, which yields more sensitive results. The target enzyme for treating depression, the MAO-A enzyme, whose 2Z5X coding structure was derived from humans, was employed in docking research. The three dimensional structures of Isoquercitrin (-8.2 kcal/mol), Rutin (-9.3 kcal/mol), Fisetin (-8.2 kcal/mol), Chrysin (-9.4 kcal/mol), Quercetin (-10.6 kcal/mol), Naringenin (8.8 kcal/mol), Kaemferol (-10.8 kcal/mol) and Luteolin (-10.8 kcal/mol) were optimized in the Gaussian09 program using the DFT/B3LYP/6-31G(d,p) basis set. Then, binding energies of these structures were determined with the help of the AutoDock Vina software. Their binding energies have been shown to indicate that they possess the property of MAO-A inhibitors.
Keywords: AgNPs, Green synthesis, Docking, *Lactifluus bertillonii*, MAO-A enzyme

Lactifluus Bertillonii Mantarından Sentezlenen Gümüş Nano Partiküllerinin Karakterizasyonu, Antimikrobiyal Aktivitesinin Belirlenmesi Ve Moleküler Modelleme Yöntemi İle MAO-A Inhıbıtor Özelliklerinin İncelenmesi

ÖZET

Bu çalışma, minimum inhibitör konsantrasyon (MIC) yöntemi kullanılarak *Lactifluus bertillonii* mantarlarından yeşil, çevre dostu bir sentez işlemi kullanılarak üretilen AgNP'lerin antimikrobiyal aktivitesine odaklanmaktadır. Ayrıca mantar ekstraktında bulunan kimyasalların inhibitör özellikleri de belirlenmiştir. Çalışmanın bir parçası olarak SEM, TEM, UV-vis ve FT-IR cihazları kullanılmıştır. Karakterizasyondaki ortalama parçacık boyutu, görüntüleme programı tarafından partikül boyutu 10.471 nm olarak belirlendi. Ayrıca MIC yöntemi kullanılarak yapılan antimikrobiyal aktivite testlerinde AgNP'lerin *Klebsiella pneumoniae*'ye karşı aktivitesinin 512 μg/ml olması daha hassas sonuçlar vermektedir. Depresyon tedavisinde hedef enzim olan ve 2Z5X kodlama yapısı insanlardan türetilen MAO-A enzimi, kenetlenme araştırmasında kullanıldı. Isoquercitrin (-8,2 kcal/mol), Rutin (-9,3 kcal/mol), Fisetin (-8,2 kcal/mol), Chrysin (-9,4 kcal/mol), Quercetin (-10,6 kcal/mol), Naringenin (8,8 kcal/mol), Kaemferol (-10,8 kcal/mol) ve Luteolin (-10,8 kcal/mol) üç boyutlu yapıları, DFT/B3LYP/6-31G(d,p) temel seti kullanılarak Gaussian 09 programında optimize edildi. Daha sonra AutoDock Vina yazılımı yardımıyla bu yapıların bağlanma enerjileri belirlendi. Bağlanma enerjilerinin MAO-A inhibitörleri özelliğine sahip olduklarını gösterdiği gösterilmiştir.

Anahtar Kelimeler: *AgNP'ler, Yeşil sentez, Docking, Lactifluus Bertillonii, MAO-A enzimi*

I. INTRODUCTION

Nanotechnology refers to research done on the nanoscale that provides shape and dimensional controls for the synthesis, description, and implementation of structures [1]. The most active areas of study and research in materials science are those related to nanotechnology. Furthermore, there is a growing global need for the synthesis of nanostructures. Structures with novel or better properties are generated by accounting for the unique properties of nanoparticles in terms of size (roughly: 1-100 nm), shape, and structure [2–4].

The fact that nanostructures have these dimensions allows them to be integrated into many fields (such as nanoscience in the energy, optoelectronics, biomedicine and biotechnology sectors) [5]. However, due to the unique development process of this rapidly developing technology, it has received more attention in the last 10 years and has many more application areas [6] (Kurnaz Yetim et al.,2021(a),2022(b)).

Nanomaterials, which have many application areas in nature, can be synthesized either synthetically or naturally from naturally occurring plants or synthetic materials. Natural materials called naturally synthesized nanoparticles can be produced naturally in nanotechnology [7]. In addition, nanoparticles synthesized by natural methods can also be metal-based. The most demanded of these are AgNPs. AgNPs are inorganic structures with diameters varying between approximately (1-100 nm) [8], and their different physical, chemical and biological properties have been the subject of many studies [9-11].

Many plants are preferred in the synthesis of metal-based nature-friendly nanoparticles by natural methods. In this study, *Lactifluus bertillonii* mushroom was preferred. In summer and fall, *Lactifluus bertillonii (Neuhoff ex Z. Schaef.)* is found in broad-leaved forests next to Fagus sp. and infrequently *Quercus sp.* It typically grows on humus-rich soils, next to *Betula sp.* and *Castanea sp.* [12]. There are many literature studies on the identification and general characteristics of the species [13-15].

The verbeken *Gastrodia bertillonii*, which is the subject of the study, is available in several provinces of our country. These provinces include Hakkari [16], Sakarya [17], Karabük [18]. Yalova [17], Rize

[19], Trabzon [20] and Gümüşhane [21]. The Turkish name of the edible mushroom is Aksütlüce, according to the literature, it was determined by [22] in the Checklist of Mushrooms of Turkey book dated 2020.

In the literature research on this mushroom species, which is included in the checklist, such a study was needed because no antimicrobial or content studies have been conducted on this mushroom before in our country. In addition, this study was designed with economic and efficiency contributions in mind. The scope of the study included testing the antimicrobial activity of AgNP particles obtained by green synthesis against some microorganisms and docking studies of the compounds determined in the LC-MS-MS device of the mushroom extract. There are many metal supported nanoparticles in the literature. After AgNPs emerged from these particles, they opened the doors to many fields. These; AgNPs are used for targeted drug delivery [23], antimicrobial [24], anti-cancer [25], antituberculosis [24], [26], [27].

II. MATERIAL AND METHOD

MATERIAL

Silver nitrate (AgNO$_3$),ultra pure wateri,filter paper(125 mm) was purchased from Sigma–Aldrich with 99.5% purity.

CHARACTERIZATION OF THE SYNTHESIZED AGNPS

The characterization analyses of AgNPs were made with FT-IR, UV-vis, TEM SEM, and energy-dispersive X-ray spectroscopy (EDX) analyzer. In characterizations, FHitachi Regulus 8230 FE-SEM(10kV, X100) model device was used for FE-SEM and FESEM-EDX. We employed the Hitachi HT7800 type TEM apparatus in this characterization step. The imaging process was carried out at 200000X, 100kV of voltage. The FT-IR devices employed were the Agilent Cary 630 FT-IR and the PerkinElmer Spectrum Two (KBr) models. The Cary 60 UV-vis Spectrophotometer was used as a model instrument for spectroscopic investigations.

METHOD

A. STUDIES ON MUSHROOM EXTRACTS

Lactifluus bertillonii was taken, properly cleaned in pure water, and then incubated for one day at a low temperature (35°C) in an oven. Using a blender, samples of mushrooms were removed from the oven and finely diced. After that, the shredded mushrooms were put in a 250 ml conical flask with 100 ml of pure water, covered with aluminum foil, heated to between 100 and 105°C for 20 minutes, and left to spin constantly in a magnetic stirrer. Following a 20-minute incubation period, the fungal sample in the conical flask was filtered through filter paper with a 0.22 mm pore size in a 250 ml conical flask that had been previously prepared. After the filtration process was complete, the filtrate was kept at +4°C for further use [28].

B. SYNTHESIS OF AGNPS PARTICLES

In a 250 ml conical flask filled with pure water, 10 mM 100 ml AgNO$_3$ solution was made. The AgNO$_3$ solution was mixed with 80 ml of previously stored mushroom extract, thoroughly covered with aluminum foil, and stirred at 250 rpm for 13 hours at 25°C using a magnetic stirrer. The centrifugation procedure was then initiated. The process of washing involved pouring pure water to the centrifuge twice, followed by one addition of either methyl or ethyl alcohol (3000 rpm, 10 minutes). In order to

use it for characterizations, the solid sample was finally fully dried in an oven set at 60ºC for a full day. The creation of AgNPs is indicated by the reaction mixture turning gray in color [29], [30].

C. ANTIMICROBIAL ACTIVITY STUDIES

C. 1. Antimicrobial activity

Using the broth microdilution method, the Minimum Inhibitory Concentration (MIC) of NPs was ascertained in 96-well U-bottom microplates. Each well received 100 µL of Brain Heart Infusion Broth. By filling the wells with 100 µL of AgNPs at a concentration of 1024 µg/ml, a twofold serial dilution was created. The negative control did not receive any nanoparticle additions. The study employed standard strains of the following bacteria: *Escherichia coli (E. coli)* ATCC 25922, *Pseudomonas aureginosa* (*P. aureginosa*) ATCC 27853, *Klebsiella pneumoniae (K. pneumoniae)* ATCC 700603, and *Staphylococcus aureus (S. aureus)* ATCC 25923. Two subcultures of the -80°C stock of bacteria were used. Using a 0.9% NaCl solution, a bacterial suspension with a McFarland turbidity of 0.5 was created from the growing colonies and diluted 1:10. Five microliters of the diluted bacterial suspension were added to each well, with the exception of the last one. Sterility control measures were taken for the final well. For twenty-four hours, microplates were incubated at 37°C. MIC is the concentration at which no discernible growth happens [31].

Antimicrobial activity was observed against gram-positive and gram-negative standard strains (Table 3).

III. RESULTS AND DISCUSSION

A. Field-Emission Scanning Electron Microscopy (FE-SEM) and Energydispersive X-ray (EDX)

The characterisation imaging shows that AgNPs particles have a slightly spherical form, however the observed picture is lump-shaped rather than distributed. Furthermore, the EDX detector revealed that the Ag element was heavier than the other elements by weight % [32–34] (Fig. 1).
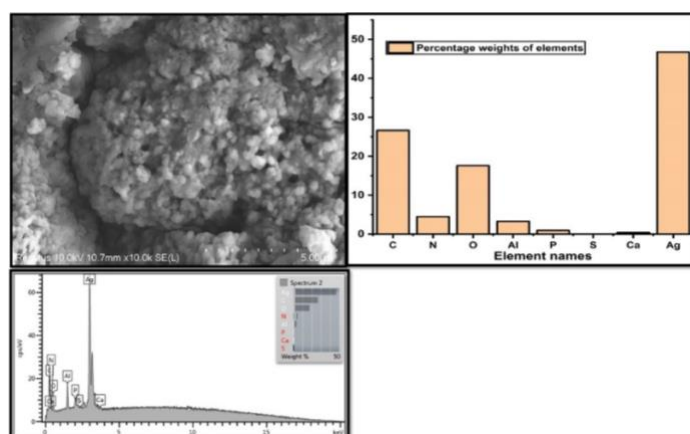

Figure 1. Shows an image of AgNPs' FESEM and EDS results

B. Transmission electron microscopy (TEM)

Both the imaging done with the TEM instrument and the particle size determination completed with the Image program yielded an average particle size of 7.12 nm. Furthermore, it was noted that the particles were generally spherical [32–34] (Fig. 2).
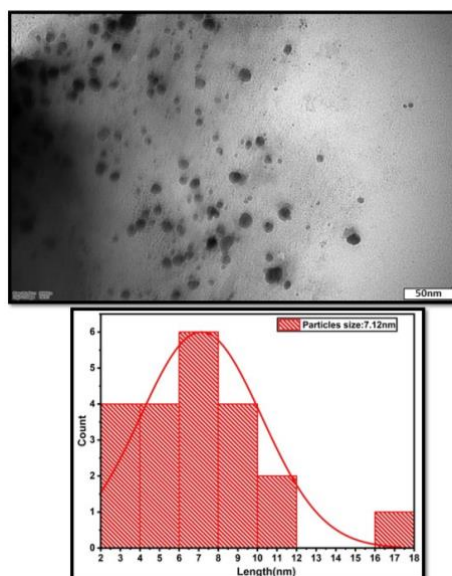
Figure 2. AgNPs TEM image and histogram of the size of particles

C. Fouirer Transform Infrared Spektrofotometre (FT-IR)

According to the spectra of the FT-IR device; the vibration band obtained at (3313 cm^{-1}) was associated with (OH) or (NH$_2$) groups, and the vibration band obtained at (1636 cm^{-1}) (C=O) was associated with carbonyl groups (extract). On the other hand, the vibration band obtained at (3292cm^{-1}) is associated with amine groups (NH$_2$), the vibration band obtained at (1582cm^{-1}) is associated with carbonyl groups (C=O), the vibration band obtained at (1394cm^{-1}) is associated with (C-H) groups, and the vibration band obtained at (1067cm^{-1}) is associated with carbonyl groups (C=O)(AgNPs). It is associated with AgNPs [32-35] (Karunakaran et al.,2017)(Fig. 3).
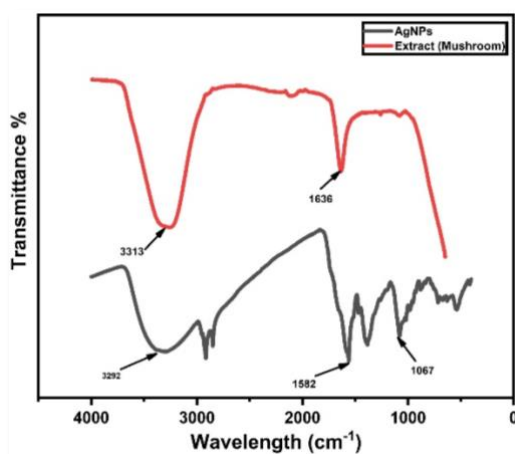

Figure 3. Image of FT-IR results of extract andAgNPs.

D. Ultraviolet–visible spectroscopy (UV-vis)

UV-vis spectroscopy is a crucial technique that is favored for assessing the stability and production of metal nanoparticles in aqueous solution [36]. The imaging done in Figure 4 using UV-vis is related to the AgNPs that were extracted from the mushroom extract. Partial parallels between AgNPs' and the extract's UV-vis spectra are observed in imaging. Nevertheless, AgNPs exhibit a single peak at 314 nm in adsorbance spectroscopy, in contrast to the *Lactifluus Bertillonii* mushroom extract [37] (Fig. 4).
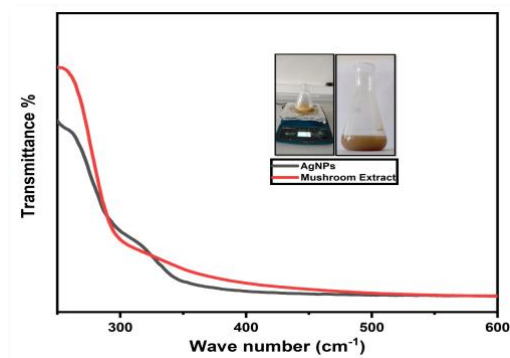
***Figure 4.*** *Image of UV-vis spectra of AgNPs and extract.*

E. LC-MS/MS

LC-MS/MS (Agilent Technologies 1260 Infinity II, 6460 Triple Quad Mass spectrometer) was used to quantify the phenolics. The employed column was a Poroshell 120 SB-C18 (3.0 × 100 mm, I.D., 2.7 μm) [38]. Samples were taken in 2 ml Eppendorf flasks containing 50 mg. To dissolve them, one milliliter of methanol was added. One milliliter of hexane was added to the final mixture to carry out the extraction process. After that, it was centrifuged for ten minutes at 9,000 rpm. Following centrifugation, 100 µl of the methanol phase was removed, and 900 µl of water was added to 450 µl of methanol. The final step was performing LC-MS/MS analysis following a 0.25 filter. Injection Volume: 5.12 ml, Flow: 0.400 mL/min, Method time: 30.00 min, Temperature: 40.00°C (Table 1).

Table 1. *Operating conditions of the LC-MS-MS device*

	Time	**A**	**B**
1	3.00 min	75.0 %	25.0 %
2	12.00 min	50.0 %	50.0 %
3	16.00 min	10.0 %	90.0 %
4	21.00 min	10.0 %	90.0 %

Included are the spectra of the substances discovered during the LC-MS/MS device examination. Protocatechuic acid, gallic acid, and catechin were among the substances whose spectra matched (Fig. 5). In addition, the table lists the chemicals that were discovered during analysis on the LC-MS/MS instrument ((Table 2).
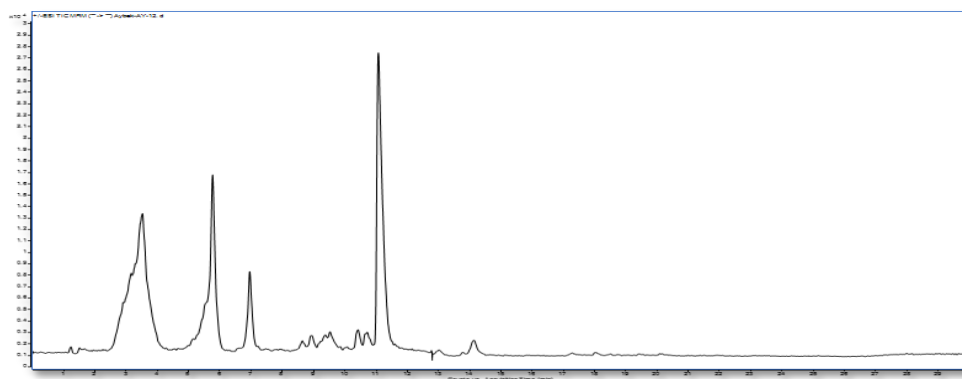
Figure 5. *Spectrum of the LC-MS-MS device.*

Table 2. *Compounds determined as a result of analysis of mushroom extract in LC-MS-MS device*

Compound Names	RT	Amount(ng/ul)
Shikimic acid	1.4296333	0.341397988
Gallic acid	3.2915167	0.32041607
Protocatechuic acid	5.4591333	0.018076958
Catechin	6.8567667	ND
Chlorogenic acid	7.1928833	0.003179637
Hydroxybenzaldeyde	7.61065	0.001271725
Vanillic acid	7.5860333	0.043874544
Caffeic acid	7.5697167	0.001052569
Syringic acid	8.3043	0.045838089
Caffein	7.9188167	ND
Vanillin	8.2475667	0.002896645
o-coumaric acid	8.96295	0.009132779
Salicylic acid	9.5659333	0.015564528
Taxifolin	9.77195	ND
Polydatin	10.006167	ND
Resveratrol	10.038133	ND
trans-ferulic acid	9.6421	0.003842722
Sinapic acid	10.024917	0.003444458
Scutellarin	11.445183	3.01026E-05
p-coumaric acid	11.45035	0.001322248
Coumarin	11.4783	ND
Protocatehuic ethyl ester	11.331883	ND
Hesperidin	11.233083	ND
Isoquercitrin	11.272883	0.258642402
Rutin	12.148267	ND
Quarcetin-3-xyloside	12.715017	ND
Kaempferol-3-glucoside	13.535217	ND
Fisetin	13.5793	ND
Baicalin	13.695583	ND
Chrysin	14.2379	ND
Compound	RT	ND
trans-cinnamic acid	14.305933	ND
Quercetin	14.905533	ND
Naringenin	14.69595	ND
Hesperetin	15.78115	ND
Morin	15.8615	ND
Kaempferol	16.338033	ND
Baicalein	17.143367	ND
Luteolin	17.833367	ND
Biochanin A	17.901083	ND
Capcaicin	17.966817	ND
Dihydrocapcaicin	18.497117	ND
Diosgenin	23.5672	ND

F. Antimicrobial activity result

Table 3. *Antimicrobial activity results according to MIC method*

Mikroorganizma	AgNPs
Staphylococcus aureus	256 µg/ml
E. coli	128 µg/ml
Klebsiella pneumoniae	512 µg/ml
Pseudomonas aeruginosa	256 µg/ml

E. EXAMINATION OF MAO-A INHIBITOR PROPERTIES USING MOLECULAR MODELING METHOD

E. 1. MAO-A enzyme and depression

MAO-A enzyme plays a major role in psychiatric diseases and depression, which is a neurological disease. For this reason, MAO-A enzyme can be considered as a drug target in the treatment of depression. Inhibitors of the MAO-A enzyme block serotonin reactions. In addition, MAO-A inhibitors have the ability to block norepinephrine and dopamine reactions and therefore can be used in the treatment of depression. MAO inhibitors have been used as antidepressants for approximately 60 years [39]. Studies suggest that depression is caused by a reduction in the necessary amounts of dopamine, serotonin, and noradrenaline in the brain. Inhibiting the MAO-A enzyme may be one way to treat depression since it is believed that raising the amount of these neurotransmitter chemicals aids in treating the condition. MAO-A inhibitors are medications that function by utilizing this mechanism [40]. FAD and cysteine are covalently bound in the MAO-A enzyme. The outer mitochondrial membrane of the lungs, liver cells, platelets, intestinal mucosa, and serotonergic nerve terminals are also heavily linked to the MAO-A enzyme. The deamination reaction of biological amines like tyramine and neurotransmitters like noradrenaline, dopamine, and serotonin is brought on by the MAO-A enzyme. The FAD coenzyme and two of the water molecules are covalently bound. The reversible and irreversible interactions of drug candidates and pharmaceuticals with amino acids in the active site of the enzyme are largely influenced by water molecules present in the active site [41].

The reason for docking with MAO-A in this study was to understand the effects of the compounds or structural features that form the basis of the research on the MAO-A enzyme and to evaluate their potential therapeutic applications. At the same time, it is likely that this study will shed light on future studies aiming to combine structures that have antimicrobial effects with a compound or material that can potentially be used in different therapeutic areas.

The docking analysis of the molecular modeling procedure carried out in this study included the following steps:

Selection of MAO-A enzyme:
The Protein Data Bank database was utilized to evaluate MAO-A enzymes that are derived from humans. The 2Z5X coded MAO-A enzyme structure was chosen for the investigation because it had the best resolution value and was mutation-free. The AutoDock Vina Program's appropriateness for docking research has been proven, and it has been verified for human MAO-A Enzyme (considering those with RMSD values less than 2 A^0) [42].

Docking preparation of some of the flavonoid structures present in the *Lactifluus bertillonii* mushroom extract:

Relevant flavonoid structures (Isoquercitrin, Rutin, Fisetin, Chrysin, Quercetin, Naringenin, Kaemferol and Luteolin) discovered in the *Lactifluus bertillonii mushroom* extract were downloaded from the PUBCHEM website in .sdf format. In order to prepare these structures for docking procedures, first the .sdf structures were converted to .gjf format with Gaussview. As a next step, .gjf format files were opened with the Gaussview interface and geometry optimizations were made in the gas phase using Gaussian09 software in the 6-31G(d,p) basis set at DFT/B3LYP level[43].

Carrying Out Doking Validation Tasks:

Validation of the docking method was carried out by placing the ligands in a data set into the enzyme using different docking programs and examining the deviation of the resulting conformations from the conformation in the original X-ray structure.

Once the 2Z5X structure was selected, the FAD cofactor was not removed from the structure because it is covalently bound to the enzyme and functions in enzyme activity. However, the Harmine (HRM)

ligand was separated from the structure. In addition, Glycerol (GOL) and Dimethyl Phosphine Oxide (DCX) ligands in the structure are also removed from the structure because they are impurities resulting from crystallization for X-ray analysis.

has been removed. Finally, all water molecules except 7 water molecules in the active site, which play an important role in binding, were deleted. Validation of the docking method is carried out by removing the ligand in the enzyme in the X-ray structure and reinserting it into the same enzyme molecule with the help of the docking program and examining the deviation of the resulting conformations from the conformation in the reference structure. For validation in the study, the HRM ligand in the 2Z5X structure was used. Human MAO-A was reconstituted using the enzyme-extracted HRM ligand AutoDock Vina.

docking was done with enzyme. All conformations found as a result of validation were also examined using the ADT user interface program. Can occur in all conformations

Electrostatic interactions and hydrogen bonds were observed thanks to the program. Of the 7 possible conformations, the 1st conformation is the one that gives significant results and has the most appropriate RMSD value. The overlapping shape of the first two best conformations found and the HRM ligand taken as reference can be seen in Figure 6.
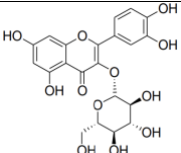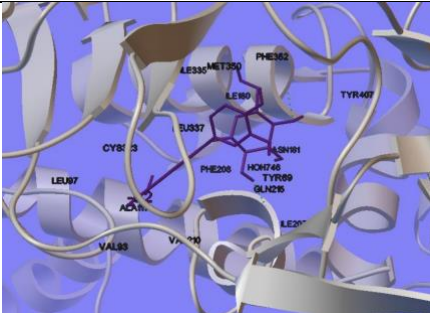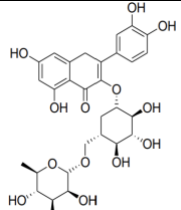

Figure 6. Validation Result (pink ligand reference, green ligand best RMSD ligand having value) RMSD= 0.89 A0

Carrying Out Doking Tasks:

Using the Autodock Vina user interface, Pdbqt files for the MAO-A enzyme and the pertinent flavonoid structures discovered in the *Lactifluus bertillonii* mushroom extract were created. A configuration file called config.txt was created in preparation for the docking process. It contained parameters that were defined as the Cartesian coordinates of the active region that needed to be docked and the area that covered the MAO-A enzyme. The grid coordinates in the config file are selected as 27x27x27. The only file used for docking procedures is the configuration file. With the aid of AutoDock Tools, the program's interface, the values in the configuration file and the MAO-A enzyme were maintained constant for every flavonoid under investigation during the docking calculations with AutoDock Vina. All flavonoids were computed using this file, and the binding energies of the chosen flavonoid structures were determined. Hydrogen bonds and other interactions, if any, were also analyzed in addition to binding energies (Table 4).
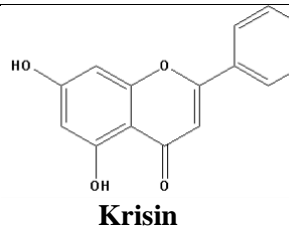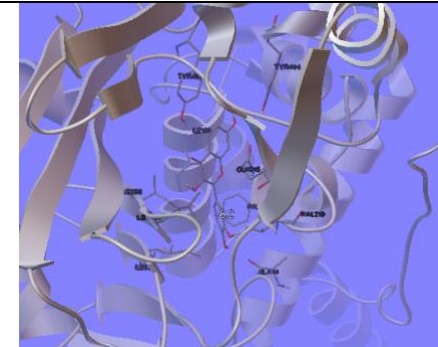
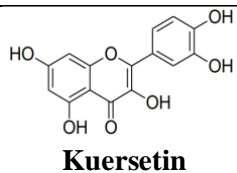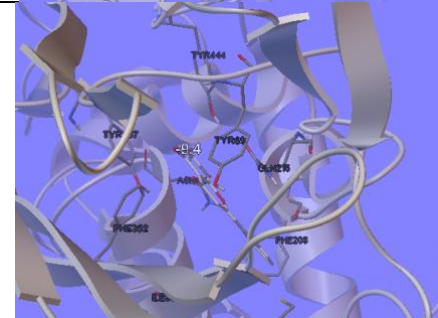| Flavonoid Structure	Binding Energy (kcal/mol)	Hydrogen Bonding and Other Interactions	Images After Doking
İzokuersitrin	-8.2	Upon analyzing the docking results, it was seen that the isoquercitrin flavonoid's most appropriate conformation was entirely situated within the active site. Van der Walls also interacts with amino acids ASN181, ILE335, GLN215, PHE352, PHE208, TYR407, VAL93, TYR69, ILE180, LEU337, CYS323, VAL210, LEU97, MET350, ILE207, and ALA111 in addition to the water molecule HOH746 that is present in the active site pocket. interacts with, as observed. Additionally, two H bonds are formed by the conformation at the active site.	
Rutin	-9.3	The binding potential of rutin flavonoid was determined to be fairly good based on docking experiments. It has been noted that the active site amino acids HOH726 and HOH805 interact with the Rutin flavonoid in its most configuration. LEU337, ILE335, TYR407, VAL210, VAL93, PHE208, GLY322, ASN92, VAL91, CYS321, ALA111, TYR69, CYS323, LEU97, PHE352, GLY110, GLN215, MET350, and SER209 amino acids are also included. The Van der Waals interaction has been noted to exist with. The active site pocket contains the matching conformation. Four H bonds are formed by the conformation in the active site. There are also pi-pi interactions in the active site.	
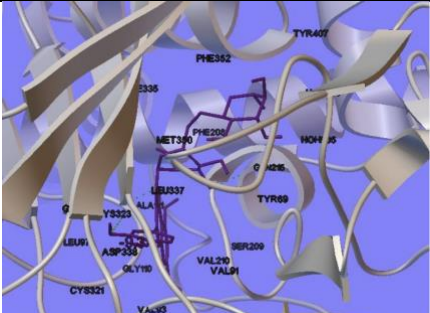
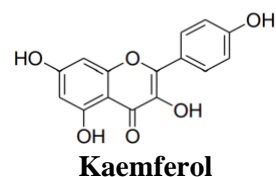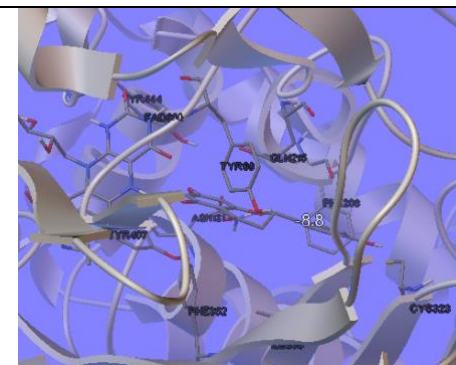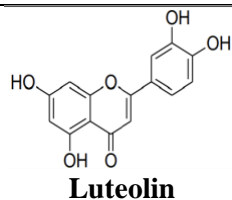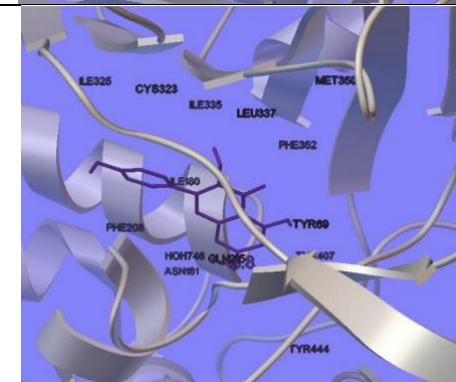|			
Fisetin	-8.2	Upon examining the proper structure of fisetin flavonoid, docking experiments revealed that it interacted with the following amino acids in the active site: TYR444, TYR407, ILE180, GLN217, LEU337, PHE208, VAL210, ALA111, and ILE325. The appropriate conformation has been found to interact with the amino acids in the active site and is situated there.	
Krisin	-9.4	The Van der Waals contact between the conformation and the amino acids PHE352, ILE335, TYR407, ASN181, TYR444, TYR69, CYS 323, GLN215, and PHE208 in the active region was observed in the docking data. Furthermore, it was shown that the active area pocket contained the proper shape. In the active area, the conformation forms a single H bond. There are also pi-pi interactions in the active site.	
Kuersetin	-10.6	The docking results showed that the quercetin molecule interacted with the water molecules HOH746; HOH739; and HOH726 in the active site in the proper conformation. Moreover, amino acids GLN215, MET350, PHE352, ILE335, FAD600, ILE325, TYR444, CYS323, VAL210, TYR69, TYR407, PHE208, and LEU337—all of which are found in the active region—were also shown to interact Van der Waals. It was noted that the active region included one H bond formed by the appropriate conformation, which was positioned there.	

2043
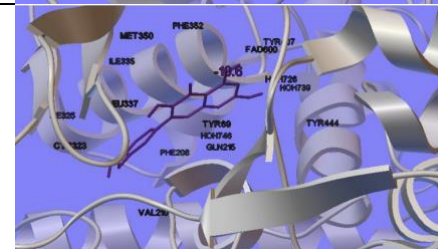
|			
 Naringenin	-8.8	Type A conformation's active site amino acids are TYR69, GLN215, TYR444, TYR407, PHE352, ASN181, CYS323, and ILE335. Furthermore, there was interaction with FAD600 as well. Examining the placement status reveals that the active region contains all of the Naringenin conformation, which interacts with the amino acids there through a Van der Waals interaction.	
 Kaemferol	-10.8	Upon analyzing the docking results of the optimal conformation of kaemferol flavonoid, it was shown that hydrogen bonds were not formed within the active site. In the active region of the conformation, a van der Waals contact has been noted. The contact is caused by two water molecules (HOH726 and HOH746). PHE208, PHE352, ASN181, ILE325, TYR69, LEU337, TYR407, ILE180, TYR444, MET350, CYS323, GLN215, and ILE335 are the amino acids that are in charge of the interaction. There are also pi-pi interactions in the active site.	
 Luteolin	-10.8	The van der Waals interactions were found to be caused by the water molecules HOH746, HOH739, and HOH726 when the conformation of luteolin in the active site was investigated. TYR444, TYR69, CYS323, LEU337, FAD600, VAL210, PHE352, ILE325, TYR407, GLN215, PHE208, ILE335, and MET350 are the amino acids that are accountable for the same interaction. In the active site, the structure forms a single H bond. There are also pi-pi interactions in the active site.	
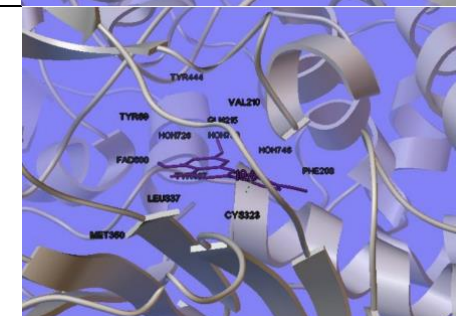
IV. CONCLUSION

Flavonoids;   It is a group of compounds known as the metabolite class, which attracts a lot of attention, creates excitement and has beneficial health benefits. It has been reported to have numerous essential biological properties, including anti-inflammatory, antibacterial, antiviral, antioxidant, and anti-cancer [44,45]. In this research, the type and amount of bioactive components in the extract of the preferred mushroom Lactifluus Bertillonii were determined. In the content analysis, gallic acid and shikimic acid were found to be the compounds with the highest concentration. Research has shown that flavonoids have biological activity in addition to their physiological roles in plants.

Docking studies were used in linked research to investigate the MAO-A enzyme inhibitory activities of various flavonoids in Lactifluus Bertillonii mushroom extract. Following docking tests, -8.2 kcal/mol to -10.8 kcal/mol for Isoquercitrin (-8.2 kcal/mol), Rutin (-9.3 kcal/mol) and Fisetin (-8.2 kcal/mol). Binding energies ranging from mol were determined. in essence. Flavonoids luteolin (-10.8 kcal/mol), kaemferol (-10.8 kcal/mol), naringenin (-8.8 kcal/mol), cherysin (-9.4 kcal/mol) via van der wall interactions and H bonds. mol) and quercetin (-9.4 kcal/mol) -10.6 kcal/mol) are located in the active site.

As a result of the study, we believe that a method has been developed that is economical and does not leave residues with side effects on the earth. In addition, since the fungal species is not widely reported in the literature and based on the characterization analysis, we think that the particle produced at the nanoscale will work in the same way with antibiotics and other drugs in pharmaceutical and other application areas. Furthermore,MAO-A enzyme docking study was carried out in order to obtain information about multiple targets as well as the antimicrobial effect. It was also evaluated whether Silver Nano Particles Synthesized from Lactifluus Bertillonii Mushroom would have neuroprotective or antidepressant properties. It is thought that the results will contribute to the field of multi-target drug design, which has attracted attention recently.

V. REFERENCES

[1]   V. Sarsar, K.K. Selwal and M.K. Selwal, "Green synthesis of silver nanoparticles using leaf extract of Mangifera indica and evaluation of their antimicrobial activity", J Microbiol Biotech Res, vol. 5, no. 3, pp. 27–32, 2013.

[2]   R. M. Slawson, J. T. Trevors, and H. Lee, "Silver accumulation and resistance in Pseudomonas stutzeri", Arch. Microbiol., vol. 158, no. 6, pp. 398–404, Nov. 1992.

[3]   H. Nalwa, 'Handbook of nanostructured materials and nanotechnology, five-volume set', 1999.

[4]   W. Jahn, "Chemical aspects of the use of gold clusters in structural biology", J. Struct. Biol., vol. 2, no. 127, pp. 106–112, 1999.

[5]   M. Zannotti, V. Vicomandi, A. Rossi, M. Minicucci, S. Ferraro, L. Petetta, and R. Giovannetti "Tuning of hydrogen peroxide etching during the synthesis of silver nanoparticles. An application of triangular nanoplates as plasmon sensors for Hg^{2+} in", J. Mol. Liq., vol. 309, p. 113238, 2020.

[6]   M.A. Kakakhel, W. Sajjad, F. Wu, N. Bibi, K. Shah, Z. Yali and W. Wang, "Green synthesis of silver nanoparticles and their shortcomings, animal blood a potential source for silver nanoparticles: A review", J. Hazard. Mater. Adv., vol. 1, p. 100005, 2021.

[7]   R. Magaye and J. Zhao, "Recent progress in studies of metallic nickel and nickel-based nanoparticles' genotoxicity and carcinogenicity", Environ. Toxicol. Pharmacol., vol. 3, no. 34, pp. 644–650, 2012.

[8]   K. Maaz, "Silver Nanoparticles: Fabrication, Characterization and Applications", IntechOpen, 2018.

[9]   L. Wang, T. Zhang, P. Li, W. Huang, J. Tang, P. Wang, J. Liu, Q. Yuan, R. Bai, B. Li, K. Zhang, Y. Zhao and C. Chen, "Use of synchrotron radiation-analytical techniques to reveal chemical origin of silver-nanoparticle cytotoxicity", ACS Publ., vol. 9, no. 6, pp. 6532–6547, Jun. 2015.

[10]   A. Syafiuddin, M. Razman Salim, A. Beng Hong Kueh, T. Hadibarata, and H. Nur, "A review of silver nanoparticles: research trends, global consumption, synthesis, properties, and future challenges", J. Chinese Chem. Soc., vol. 64, no. 7, pp. 732–756, Jul. 2017.

[11]   M. Köktürk, A. Yiğit and E. Sulukan, "Green Synthesis Iron Oxide Nanoparticles (Fe@ AV NPs) Induce Developmental Toxicity and Anxiety-Like Behavior in Zebrafish Embryo-Larvae", Mar. Sci. Technol. Bull., vol. 12, no. 1, pp. 39–50, 2023.

[12]   F., Kränzlin, "Fungi of Switzerland: english translation: Virginia L. Waters: a contribution to the knowledge of the fungal flora of Switzerland.", Mykologia, 2005. [Online]. Available: https://scholar.google.com/scholar?hl=tr&as_sdt=0%2C5&q=Kränzlin%2C+F.%2C+2005.+Fungi+of +Switzerland%2C+Vol.+6.+Verlag+Mykologia+Lucerne%2C+İsviçre.+320.&btnG=. [Accessed: 21-Feb-2024].

[13]   M. Caboň and S. Adamčík, "Ecology and distribution of white milkcaps in Slovakia.", Czech Mycol., vol. 2, no. 66, 2014.

[14]   Y. Tuo, N. Rong, J. Hu, G. Zhao, Y. Wang, Z. Zhang, Z. Qi, Y. Li and B. Zhang, "Exploring the relationships between macrofungi diversity and major environmental factors in Wunvfeng National Forest Park in Northeast China", J. Fungi, vol. 2, no. 8, p. 98, 2022.

[15]   X.H. Xu, A.M. Chen, N. Yao, T.C. Wen, Y. Pei and W.P. Zhang, "Three New Species of Lactifluus (Basidiomycota, Russulaceae) from Guizhou Province, Southwest China", J. Fungi, vol. 1, no. 9, p. 122, 2023.

[16]   Y. KESİCİ, S., UZUN, 'Adaklı (Yüksekova/Hakkâri) ve çevre köylerde belirlenen makromantarlar', *Mantar Derg.*, vol. 12, no. 2, pp. 148–162, 2021.

[17]   H. Dogan, Ö. Öztürk and M.A.Ş. Şanda, 'The Mycobiota of Samanli Mountains in Turkey', Trak. Univ. J. Nat. Sci., vol. 22, no. 2, pp. 215–243, 2021.

[18]   G. Kaşik, S. Alkan, S. Aktaş, C. Öztürk, and H. Esra AKGÜL, 'MacrofMacrofungi of Yenice (Karabük) District and New Records for Turkey', Kahramanmaraş Sütçü İmam Üniversitesi Tarım ve Doğa Derg., vol. 25, no. 6, pp. 1264–1278, 2022.

[19]   A. Keleş, K. Demirel, Y. Uzun, and A. Kaya, 'Macrofungi of Ayder (Rize/Turkey) high plateau', Biol. Divers. Conserv., vol. 3, no. 7, pp. 177–183, 2014.

[20]   H. Solak, M.H., Işıloğlu, M., Kalmış, and E., Allı, 'Macrofungi of Turkey: Checklist', *İzmir*, 2007.   [Online].   Available: https://scholar.google.com/scholar?hl=tr&as_sdt=0%2C5&q=Solak%2C+M.H.%2C+Işıloğlu%2C+M. %2C+Kalmış%2C+E.%2C+Allı%2C+H.+2015.+Macrofungi+of+Turkey%2C+Checklist+Volume+2. +Üniversiteliler+Ofset%2C+İzmir.&btnG=. [Accessed: 21-Feb-2024].

[21]   I. Akata, Y. Uzun, and A. Kaya, 'Macrofungal diversity of Zigana Mountain (Gümüşhane/Turkey)', 2016.

[22]   A. 2020 Sesli, E., Asan, A., Selçuk, F., Abacı Günyar, Ö., Akata, I., Akgül, S., Alkan, S., Allı, H., Aydoğdu, H., Berikten, D., Demirel, K., Demirel, R., Doğan, H. H., Erdoğdu, M., Ergül, C. C., Eroğlu, G., Giray, G., Halikî Uztan, A., Kabaktepe, Ş., Kadaifçiler, 'Türkiye mantarları listesi', İstanbul: Ali Nihat Gökyiğit Vakfı Yayını., 2020. [Online]. Available: https://scholar.google.com/scholar?hl=tr&as_sdt=0%2C5&q=Sesli%2C+E.%2C+Asan%2C+A.%2C+Selçuk%2C+F.%2C+Abacı+Günyar%2C+Ö.%2C+Akata%2C+I.%2C+Akgül%2C+S.%2C+Alkan%2C+S.%2C+Allı%2C+H.%2C+Aydoğdu%2C+H.%2C+Berikten%2C+D.%2C+Demirel%2C+K.%2C+Demirel%2C+R.%2C+Doğa. [Accessed: 21-Feb-2024].

[23]   S. S. Suri, H. Fenniri, and B. Singh, 'Nanotechnology-based drug delivery systems', J. Occup. Med. Toxicol., vol. 2, no. 1, 2007.

[24]   H. P. Borase, B.K. Salunke, R.B. Salunkhe, C.D. Patil, J.E. Hallsworth, B.S. Kim, and S.V. Patil, 'Plant extract: A promising biomatrix for ecofriendly, controlled synthesis of silver nanoparticles', Appl. Biochem. Biotechnol., vol. 173, no. 1, pp. 1–29, 2014.

[25]   K. K. Jain, 'Advances in the field of nanooncology', BMC Med., vol. 8, p. 83, Dec. 2010.

[26]   Y. V. Anisimova, S. I. Gelperina, C. A. Peloquin, and L. B. Heifets, 'Nanoparticles as antituberculosis drugs carriers: Effect on activity against Mycobacterium tuberculosis in human monocyte-derived macrophages', J. Nanoparticle Res., vol. 2, no. 2, pp. 165–171, 2000.

[27]   S. Mohanty, P. Jena, R. Mehta, R. Pati, B. Banerjee, S. Patil and A. Sonawane, 'Cationic antimicrobial peptides and biogenic silver nanoparticles kill mycobacteria without eliciting DNA damage and cytotoxicity in mouse macrophages', Am Soc Microbiol, vol. 57, no. 8, pp. 3688–3698, Aug. 2013.

[28]   H. S. Devi, M. A. Boda, M. A. Shah, S. Parveen, and A. H. Wani, 'Green synthesis of iron oxide nanoparticles using Platanus orientalis leaf extract for antifungal activity', Green Process. Synth., vol. 8, no. 1, pp. 38–45, Jan. 2019.

[29]   D. Ozturk, A. Ozguven, V. Yonten, and M. Ertas, 'Green synthesis, characterization and antimicrobial activity of silver nanoparticles using Ornithogalum narbonense L.', Inorg. Nano-Metal Chem., vol. 52, no. 3, pp. 329–341, 2022.

[30]   E. N. Gecer, R. Erenler, C. Temiz, N. Genc, and I. Yildiz, 'Green synthesis of silver nanoparticles from Echinacea purpurea (L.) Moench with antioxidant profile', Part. Sci. Technol., vol. 40, no. 1, pp. 50–57, 2022.

[31]   P. A. Wayne, 'Clinical and Laboratory Standards Institute: Performance standards for antimicrobial susceptibility testing: 20th informational supplement', *CLSI Doc.* M100-S20, 2010.

[32]   G. Geoprincy, B. N. Srri, U. Poonguzhali, N. N. Gandhi, and S. Renganathan, 'A review on green synthesis of silver nanoparticles', Asian J. Pharm. Clin. Res., *6*(1), 8-12, 2013.

[33]   B. K. Salunke, J. Shin, S. S. Sawant, B. Alkotaini, S. Lee, and B. S. Kim, 'Rapid biological synthesis of silver nanoparticles using Kalopanax pictus plant extract and their antimicrobial activity', J. Chem. Eng. , vol. 31, no. 11, pp. 2035–2040, Nov. 2014.

[34]   R. Rani, D. Sharma, M. Chaturvedi, and J.P. Yadav, 'Green synthesis, characterization and antibacterial activity of silver nanoparticles of endophytic fungi Aspergillus terreus', J Nanomed Nanotechnol, vol. 4, no. 8, p. 1000457, 2017.

[35]   T. K. Dua, S. Giri, G. Nandi, R. Sahu, T. K. Shaw, and P. Paul, 'Green synthesis of silver nanoparticles using Eupatorium adenophorum leaf extract: characterizations, antioxidant, antibacterial and photocatalytic activities', Chem. Pap., vol. 77, no. 6, pp. 2947–2956, Jun. 2023.

[36]   D. Philip, C. Unni, S.A. Aromal, and V. K. Vidhu, 'Murraya koenigii leaf-assisted rapid green synthesis of silver and gold nanoparticles', Spectrochim. Acta Part A Mol. Biomol. Spectrosc., vol. 2, no. 78, pp. 899–904, 2011.

[37]   J. M. War, A. H. Wani, A. U. Nisa, and M.Y. Bhat, 'Green Synthesis, Characterization and In Vitro Antimicrobial Activity of Silver Nanoparticles (AgNPs) Using Fungal Aqueous Extract', Nano, vol. 17, no. 13, Dec. 2022.

[38]   R. Erenler, M. N. Atalar, İ. Yıldız, E.N. Geçer, A. Yıldırım, İ. Demirtaş and M.H. Alma, 'Quantitative analysis of bioactive compounds by LC-MS/MS from Inula graveolens', Bütünleyici ve Anadolu Tıbbı Derg., vol. 3, no. 4, pp. 3–10, 2023.

[39]   G. Jo, S.H. Sung, Y. Lee, B.G. Kim, J.W. Yoon, H.O. Lee, S.Y. Ji, D. Koh, J.H. Ahn and Y. Lim, 'Discovery of monoamine oxidase A inhibitors derived from in silico docking', Bull. Korean Chem. Soc., vol. 33, no. 11, p. 3841, 2012.

[40]   O. Trott, and A. Olson, 'AutoDock Vina: improving the speed and accuracy of docking with a new scoring function, efficient optimization, and multithreading', J. Comput. Chem., vol. 31, no. 2, pp. 455–461, Jan. 2010.

[41]   S. Y. Son, J. Ma, Y. Kondou, M. Yoshimura, E. Yamashita, and T. Tsukihara, 'Structure of human monoamine oxidase A at 2.2-Å resolution: The control of opening the entry for substrates/inhibitors', Proc. Natl. Acad. Sci. U. S. A., vol. 105, no. 15, pp. 5739–5744, Apr. 2008.

[42] S. Son, J. Man, Y. Kondou, M. Yoshimura, E. Yamashita and T. Tsukihara, " Structure of human monoamine oxidase A at 2.2-Å resolution: The control of opening the entry for substrates/inhibitors", *Proceedings of the National Academy of Sciences*, *105*(15), 5739-5744.

[43] Gaussian 09, Revision A.02, M. J. Frisch, G. W. Trucks, H. B. Schlegel, G. E. Scuseria, M. A. Robb, J. R. Cheeseman, G. Scalmani, V. Barone, G. A. Petersson, H. Nakatsuji, X. Li, M. Caricato, A. Marenich, J. Bloino, B. G. Janesko, R. Gomperts, B. Mennucci, H. P. Hratchian, J. V. Ortiz, A. F. Izmaylov, J. L. Sonnenberg, D. Williams-Young, F. Ding, F. Lipparini, F. Egidi, J. Goings, B. Peng, A. Petrone, T. Henderson, D. Ranasinghe, V. G. Zakrzewski, J. Gao, N. Rega, G. Zheng, W. Liang, M. Hada, M. Ehara, K. Toyota, R. Fukuda, J. Hasegawa, M. Ishida, T. Nakajima, Y. Honda, O. Kitao, H. Nakai, T. Vreven, K. Throssell, J. A. Montgomery, Jr., J. E. Peralta, F. Ogliaro, M. Bearpark, J. J. Heyd, E. Brothers, K. N. Kudin, V. N. Staroverov, T. Keith, R. Kobayashi, J. Normand, K. Raghavachari, A. Rendell, J. C. Burant, S. S. Iyengar, J. Tomasi, M. Cossi, J. M. Millam, M. Klene, C. Adamo, R. Cammi, J. W. Ochterski, R. L. Martin, K. Morokuma, O. Farkas, J. B. Foresman, and D. J. Fox, Gaussian, Inc., Wallingford CT, 2016.

[44]   R. Erenler, Ü. Çarlık, and A. Aydın, 'Antiproliferative activity and cytotoxic effect of essential oil and water extract from origanum Vulgare L.', Sigma, vol. 1, no. 41, pp. 202–208, 2023.
[45]   Y. Keşkek, 'Kantaron flavonoidlerinin moleküler modelleme ve deneysel çalışmalar ile depresyon tedavisinde kullanılacak yeni mao-a inhibitörlerinin tasarlanması', *(Master's thesis, Fen Bilimleri Enstitüsü).*, 2016. [Online]. Available: https://scholar.google.com/scholar?hl=tr&as_sdt=0%2C5&q=Kantaron+flavonoidlerinin+moleküler+

modelleme+ve+deneysel+çalışmalar+ile+depresyon+tedavisinde+kullanılacak+yeni+mao-a+inhibitörlerinin+tasarlanması.+MS+thesis.+Fen+Bilimleri+Enstitüsü%2C+2016.&btnG=. [Accessed: 21-Feb-2024].

[46]   N. Kurnaz Yetim, M.M. Koç & D. Nartop, "Magnetic dendrimer-encapsulated metal nanoparticles (Au, Ag): effect of dendrimerization on catalytic reduction of 4-nitrophenol". Journal of the Iranian Chemical Society, 19(6), 2569-2580, 2022.

[47]   N. Kurnaz Yetim, F. Kurşun Baysak, M.M. Koç, & D. Nartop, "Synthesis and characterization of Au and Bi2O3 decorated Fe3O4@ PAMAM dendrimer nanocomposites for medical applications". Journal of Nanostructure in Chemistry, 11(4), 589-599, 2021.

[48]   Karunakaran, G., Jagathambal, M., Venkatesh, M., Kumar, G. S., Kolesnikov, E., Dmitry, A., ... & Kuznetsov, D. (2017). Hydrangea paniculata flower extract-mediated green synthesis of MgNPs and AgNPs for health care applications. Powder Technology, 305, 488-494.